Methionine Adenosyltransferase 1A Gene Deletion Disrupts Hepatic Very Low-Density Lipoprotein Assembly in Mice

ARTICLE *in* HEPATOLOGY · DECEMBER 2011

Impact Factor: 11.06 · DOI: 10.1002/hep.24607 · Source: PubMed

11 AUTHORS, INCLUDING:

Ainara Cano
One Way Liver
18 PUBLICATIONS **136** CITATIONS
SEE PROFILE

Xabier Buque
Universidad del País Vasco / Euskal Herriko U…
22 PUBLICATIONS **209** CITATIONS
SEE PROFILE

Begona Ochoa
University of the Basque Country, Leioa, Spain
113 PUBLICATIONS **1,207** CITATIONS
SEE PROFILE

Patricia Aspichueta
Universidad del País Vasco / Euskal Herriko U…
41 PUBLICATIONS **376** CITATIONS
SEE PROFILE

Methionine Adenosyltransferase 1A Gene Deletion Disrupts Hepatic Very Low-Density Lipoprotein Assembly in Mice

Ainara Cano,[1] Xabier Buqué,[1] Maite Martínez-Uña,[1] Igor Aurrekoetxea,[1] Ariane Menor,[1] Juan L. García-Rodríguez,[2] Shelly C. Lu,[3] M. Luz Martínez-Chantar,[2] José M. Mato,[2] Begoña Ochoa,[1] and Patricia Aspichueta[1]

Very low-density lipoprotein (VLDL) secretion provides a mechanism to export triglycerides (TG) from the liver to peripheral tissues, maintaining lipid homeostasis. In nonalcoholic fatty liver disease (NAFLD), VLDL secretion disturbances are unclear. Methionine adenosyltransferase (MAT) is responsible for *S*-adenosylmethionine (SAMe) synthesis and MAT I and III are the products of the *MAT1A* gene. Deficient MAT I and III activities and SAMe content in the liver have been associated with NAFLD, but whether *MAT1A* is required for normal VLDL assembly remains unknown. We investigated the role of *MAT1A* on VLDL assembly in two metabolic contexts: in 3-month-old *MAT1A*-knockout mice (3-KO), with no signs of liver injury, and in 8-month-old *MAT1A*-knockout mice (8-KO), harboring nonalcoholic steatohepatitis. In 3-KO mouse liver, there is a potent effect of *MAT1A* deletion on lipid handling, decreasing mobilization of TG stores, TG secretion in VLDL and phosphatidylcholine synthesis via phosphatidylethanolamine *N*-methyltransferase. *MAT1A* deletion also increased VLDL– apolipoprotein B secretion, leading to small, lipid-poor VLDL particles. Administration of SAMe to 3-KO mice for 7 days recovered crucial altered processes in VLDL assembly and features of the secreted lipoproteins. The unfolded protein response was activated in 8-KO mouse liver, in which TG accumulated and the phosphatidylcholine-to-phosphatidylethanolamine ratio was reduced in the endoplasmic reticulum, whereas secretion of TG and apolipoprotein B in VLDL was increased and the VLDL physical characteristics resembled that in 3-KO mice. *MAT1A* deletion also altered plasma lipid homeostasis, with an increase in lipid transport in low-density lipoprotein subclasses and decrease in high-density lipoprotein subclasses. *Conclusion: MAT1A* is required for normal VLDL assembly and plasma lipid homeostasis in mice. Impaired VLDL synthesis, mainly due to SAMe deficiency, contributes to NAFLD development in *MAT1A*-KO mice. (HEPATOLOGY 2011;54:1975-1986

Very low-density lipoprotein (VLDL) assembly is an intricate process involving multiple cellular and molecular events, some of which are still undetermined.[1] When abnormalities in the secretion of VLDL occur, lipids—mainly triglycerides (TG)—are not recruited for VLDL assembly and remain stored as cytosolic lipid droplets.[2,3] Findings regarding VLDL secretion in patients with nonalcoholic fatty liver disease (NAFLD)

Abbreviations: apo, apolipoprotein; AMPK, adenosine monophosphate–activated protein kinase; Chol, cholesterol; DGAT, diacylglycerol acyltransferase; eIF2α, α-subunit of eukaryotic initiation factor 2; ER, endoplasmic reticulum; FFA, free fatty acid; KB, ketone bodies; KO, knockout; MAT, methionine adenosyltransferase; MTP, microsomal triglyceride transfer protein; NAFLD, nonalcoholic fatty liver disease; NASH, nonalcoholic steatohepatitis; PC, phosphatidylcholine; PE, phosphatidylethanolamine; PEMT, phosphatidylethanolamine N*-methyltransferase; PERK, double-stranded RNA-activated protein kinase (PKR)-like ER kinase; qRT-PCR, quantitative real-time polymerase chain reaction; SAH,* S*-adenosylhomocysteine; SAMe,* S*-adenosylmethionine; TG, triglyceride; TGL, triglyceride lipase; VLDL, very low-density lipoprotein; WT, wild type.*

From the [1]Department of Physiology, University of the Basque Country Medical School, Bilbao, Spain; [2]CIC bioGUNE, Centro de Investigación Biomédica en Red de Enfermedades Hepáticas y Digestivas (CIBERehd), Technology Park of Bizkaia, Spain; and [3]Division of Gastroenterology and Liver Diseases, University of Southern California Research Center for Liver Diseases, Keck School of Medicine, University of Southern California, Los Angeles, California, USA.

Received April 8, 2011; accepted July 26, 2011.

This work was supported by the Basque Government IT-336-10 (to B.O. and P.A.) and Ministerio de Educación SAF2007-60211 (to B.O. and P.A.), US National Institutes of Health AT-1576 (to S.C.L., M.L.M-C. and J.M.M.), SAF2008-04800 (to M.L.M-C. and J.M.M.), and Etortek bioGUNE 2008 IE08-228 (to P.A and M.L.M-C). A.C. was a recipient of a predoctoral fellowship from the University of the Basque Country and was awarded the National Investigation prize "Juan Abelló Pascual" from the Royal Academy of Doctors of Spain (RADE).

are controversial,[4] with some studies showing that the rate of VLDL-TG secretion is increased,[5] whereas others report just the opposite.[2]

During VLDL assembly, provision of lipid is needed for the correct translation and translocation of apolipoprotein B (apoB) to the lumen of the endoplasmic reticulum (ER).[6,7] Because the majority of VLDL-TG (60%-70%) is derived from intracellular stores,[8,9,11] the mobilization of lipids from the cytosolic lipid droplets toward the ER represents a potentially regulated step in VLDL production and secretion.[9-11] Each VLDL particle contains one molecule of apoB100 (or apoB48 in rodents), and its lipidation and translocation are controlled by numerous chaperones together with the microsomal TG transfer protein (MTP), whose binding and lipid transfer activity is one of the major determinants in VLDL secretion.[12] ApoB synthesis is thought to far exceed its secretion and, in normal conditions, when lipid binding is disfavored, VLDL assembly is aborted and intracellular apoB degradation occurs by proteasomal and nonproteasomal pathways.[13,14] Conditions associated with excessive synthesis, misfolding, and accumulation of hepatic apoB in the secretory pathway have been related to the induction of ER stress and activation of the unfolded protein response (UPR),[15] which has been implicated in NAFLD pathogenesis.[16] Ota et al.[17] reported that mild ER stress secondary to increased fatty acid (FA) delivery to the liver was associated with increased secretion of apoB, whereas greater ER stress and/or the presence of ER stress for a longer period of time in response to FA delivery and/or TG accumulation resulted in reduced apoB secretion and hepatic steatosis.

VLDL assembly and secretion is strongly influenced by alterations in the *de novo* biosynthesis of phosphatidylcholine (PC).[18] Two pathways are involved in PC synthesis: the CDP-choline pathway and the phosphatidylethanolamine (PE) methylation pathway, catalyzed by phosphatidylethanolamine *N*-methyltransferase (PEMT). In animal models, both pathways are required for normal VLDL secretion.[19,20] PEMT accounts for the formation of 30% of liver PC and three *S*-adenosylmethionine (SAMe) molecules are used in this reaction. SAMe is synthesized in a reaction catalyzed by methionine adenosyltransferase (MAT). MAT I and III are the products of *MAT1A* gene and are expressed mainly in the adult liver. In patients with liver cirrhosis, both MAT I and III and PEMT activities are markedly reduced.[21,22] SAMe is an important precursor of glutathione (GSH),[23] and its use in liver disease therapy has been found to result in the restoration of hepatic GSH levels in patients with cirrhosis.[24] Most of the daily synthesized SAMe is used for the donation of methyl groups in transmethylation reactions, a process in which SAMe is converted to *S*-adenosylhomocysteine (SAH).[23] *MAT1A*-knockout (*MAT1A*-KO) mice exhibit hypermethioninemia, chronic hepatic SAMe deficiency, and low levels of GSH, but hepatic SAH and plasma total homocysteine levels are not changed.[25] The 3-month-old *MAT1A*-KO mice are more prone to develop NAFLD when fed a choline-deficient diet than control animals, and at 8 months of age spontaneously develop nonalcoholic steatohepatitis (NASH), which progresses to hepatocarcinoma by 18 months.[25]

In this context, we aimed to determine whether *MAT1A* deletion disturbs VLDL secretion in mice, and if so to identify lipid handling and ER processes that are involved in VLDL assembly and their potential implications in the development of NAFLD and the associated disturbances in plasma lipid homeostasis.

Materials and Methods

Animal Studies. The 3- and 8-month-old male *MAT1A*-KO mice and their wild-type (WT) C57BL/6 littermates were obtained from the animal facility of CIC bioGUNE. Mice were housed at 22°C with a 12-hour light–dark cycle and allowed food (Teklad Global 18% Protein Rodent Diet 2018S) and water *ad libitum*. 3-month-old mice were administered daily by oral gavage 100 mg/kg SAMe or vehicle alone for 7 days.[26] After 2 hours of food deprivation, animals were anesthetized (sodium pentobarbital, 60 mg/kg body weight, given intraperitoneally) and used for blood and liver collection or for VLDL secretion studies. Animal procedures were approved by the University of the Basque Country and CIC bioGUNE ethical committees in accordance with

Address reprint requests to: Patricia Aspichueta, Ph.D., Department of Physiology, University of the Basque Country Medical School, Sarriena s/n, 48940 Leioa, Spain. E-mail: patricia.aspichueta@ehu.es; fax: +34 946015662.

View this article online at wileyonlinelibrary.com.
DOI 10.1002/hep.24607
Potential conflict of interest: Nothing to report.
Additional Supporting Information may be found in the online version of this article.

the guidelines of European Research Council for animal care and use.

Determination of Hepatic VLDL Secretion Rate and Size. Mice were injected intraperitoneally with saline or 1 mg/g body weight poloxamer 407 (P-407) (Invitrogen, Carlsbad, CA) in saline to inhibit VLDL catabolism. Blood was collected before and 6 hours after P-407 injection, serum was extracted, and VLDL ($d < 1.02$ g/mL) were isolated by ultracentrifugation and characterized for apoB48, apoB100, cholesterol (Chol), and TG. Diameters of VLDL were estimated by dynamic light scattering (Zetasizer 4; Malvern Instruments, Malvern, UK).

Quantification of Lipids in Liver and Hepatic Microsomes. Livers (300 mg) were homogenized in ice-cold phosphate-buffered saline (PBS; 10 mM), and lipids were extracted from homogenates.[27] TG, cholesterol, and free fatty acids (FFA) were quantified with commercial kits (Cobas, Roche Applied Science; Menarini Diagnostics; and Wako Chemicals GmbH, respectively).

Microsomes were isolated from liver samples (500 mg) by serial centrifugations as detailed in the Supporting Information. Lipids were extracted from microsomes[27] separated by thin-layer chromatography, and quantified by optical densitometry as detailed elsewhere.[28]

Turnover and Secretion of Triglycerides in Primary Hepatocytes. Hepatocytes plated in 60-mm dishes at 2×10^6 cells/dish were incubated for 6 hours in Dulbecco's modified Eagle medium (DMEM) containing 15% fetal bovine serum, then washed and incubated overnight in DMEM as described.[10] Cells were then incubated in 2 mL of DMEM containing 0.4 mM [^{3}H]oleic acid (5 μCi) complexed with 0.5% fatty acid–free bovine serum albumin (BSA) and [^{14}C]glycerol (0.5 μCi). After 4 hours, cells and media were collected for analysis (pulse). Other dishes were washed with PBS and incubated for 1 hour with DMEM to allow secretion of newly synthesized lipids. Cells were then incubated 4 hours and cells and media collected for the analysis of secretion of preformed lipids (chase). Lipids were extracted,[27] separated by thin-layer chromatography,[28] and analyzed as detailed in the Supporting Information.

Immunoblot Analysis. For the analysis of apoB, LC3II, and double-stranded RNA-activated protein kinase–like endoplasmic reticulum kinase (PERK), and α-subunit of eukaryotic initiation factor 2 (eIF2α) and their phosphorylated forms, lysates were subjected to sodium dodecyl sulfate-polyacrylamide gel electrophoresis (SDS-PAGE), transferred to membranes and immunoblotted as detailed in the Supporting Information.

Activity Measurement of the Liver Microsomal Enzymes MTP, PEMT, TG Lipase, and Diacylglycerol Acyltransferase. MTP activity was measured using a fluorescence assay (Chylos, Woodbury, NY).[29] The activities of PEMT, TG lipase, and diacylglycerol acyltransferase (DGAT) were performed by radiometric assays.[30-32]

Triglycerides and Cholesterol Distribution in Serum Lipoprotein Subclasses. Serum lipoproteins were analyzed by a computer-assisted online dual enzymatic method for the simultaneous quantification of total cholesterol and TG in 20 HPLC-separated lipoprotein fractions at Skylight Biotech Inc. (Akita, Japan) according to methods described previously.[33] The particle size of lipoproteins was estimated by the elution time of the column and appropriate size markers.[33]

Statistical Analysis. Data are represented as means ± SEM using Student unpaired t test. Correlations were calculated using Pearson's correlation coefficient. Significance was defined as $P < 0.05$.

Results

Characterization of MAT1A-KO Mice. As described previously,[25] liver histology was normal in 3-KO mice but not in 8-KO animals, where NASH was evident (not shown). Compared to WT mice, 8-KO animals showed increased liver weight and TG content, liver damage, as assessed by increased aspartate aminotransferase (AST) and alanine aminotransferase (ALT) activities, and decreased serum albumin and bilirubin levels (Fig. 1A,B,D). Because liver cholesterol and serum FFA (Fig. 1C,E) levels were lower in 8-KO than in 8-WT mice, it seems that whole body lipid homeostasis is affected by chronic loss of *MAT1A*. However, 3-KO mice had normal body and liver weight, and did not exhibit altered hepatic lipid content (Fig. 1A-C) or major liver damage (Fig. 1D). Nevertheless, decreased plasma levels of glucose and FFA and increased ketone bodies (KB) in 3-KO mice (Fig. 1E) suggest that global fuel metabolism is under *MAT1A* control. To determine whether *MAT1A* is required for VLDL assembly and secretion, as well as its relationship to NAFLD development, we used 3-KO mice because at this age there are no signs of liver injury.

MAT1A Deletion Increases the Rate of VLDL-apoB Secretion and Impairs VLDL-Lipid Output in Mice. The number of VLDL (apoB) particles secreted *in vivo* by the liver was 50% higher in 3-KO mice than in 3-WT mice, mainly due to apoB100-bearing

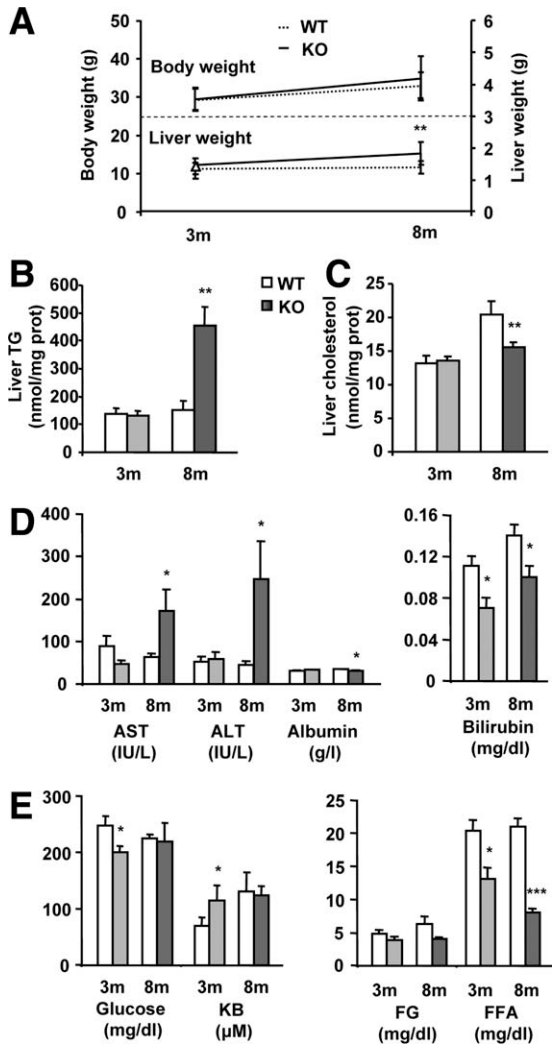

Fig. 1. Characterization of *MAT1A*-KO mice. Three-month-old (3m) and 8-month-old (8m) wild-type (WT) (□) and *MAT1A*-knockout (*MAT1A*-KO) (■) mice were used. (A) Animals were fasted 2 hours before body and liver weight estimations and blood and liver collection. Lipids were extracted from liver homogenates, and (B) triglyceride (TG) and (C) cholesterol were quantified using commercial kits as detailed in material and methods. (D) The serum activities of aspartate aminotransferase (AST) and alanine aminotransferase (ALT) and the serum levels of albumin, bilirubin, (E) glucose, ketone bodies (KB), free glycerol (FG) and free fatty acids (FFA) were measured as described in materials and methods. Values are means ± SEM of 4-8 animals per group. Statistical differences between *MAT1A*-KO and WT mice are denoted by $*P < 0.05$, $**P < 0.01$ and $***P < 0.001$ (Student *t* test).

particles, and three times higher in 8-KO mice than in 8-WT mice, due to both apoB48- and apoB100-carrying VLDL (Fig. 2A).

In 3-KO mice, 25% less TG was secreted in VLDL than in 3-WT animals, which might contribute to the accumulation of liver fat observed at 8 months, where VLDL-TG secretion increased approximately two-fold when compared to 8-WT (Fig. 2B). These findings indicate that *MAT1A* deletion promotes persistent lack of correlation between the secretion of apoB and TG in VLDL particles (Fig. 2E,F), which altered the TG to apoB ratio (reduced 43% in 3-KO and 25% in 8-KO), suggesting an impairment in the recruitment of TG for apoB lipidation and, consequently, in the composition and size of secreted VLDL particles. The latter was confirmed by dynamic light scattering of newly secreted VLDL by mice hepatocytes in culture (Fig. 2D).

The cholesterol mass secreted in VLDL (Fig. 2C) increased by 87% in 3-KO mice and decreased by 35% in 8-KO mice if compared to their respective controls, suggesting abnormalities in VLDL lipid assembly.

MAT1A Deletion Alters the Microsomal Lipid Composition in Mice. Compared to WT mice, liver microsomes from 3-KO animals contained 60% less FFA, whereas the content of other analyzed lipids was normal (Fig. 3A). In contrast, 8-KO mice liver microsomes had normal levels of FFA and of the other analyzed lipids, except for TG, which was 80% higher than in 8-WT animals (Fig. 3B), and PE, which was increased by 45% compared to their controls (Fig. 3C). The ratio PC to PE decreased by 21% in 8-KO animals whereas in 3-KO was similar to that in 3-WT mice (Fig. 3D). Nevertheless, PEMT activity (Fig. 3E) and transcript expression (Supporting Fig. 1A) were reduced by 30% and 40%, respectively, only in 3-KO mice.

MAT1A Deletion Decreases the Mobilization of TG for VLDL Secretion in 3-Month-Old Mice. DGAT and TG lipase activity (Fig. 4A,B) and the transcript expression of arylacetamide deacetylase (AADA) and triglyceride hydrolase (TGH), the main TG lipases in liver, were decreased in 3-KO mice when compared to 3-WT animals, whereas DGAT-2 transcript expression did not change (Supporting Fig. 1B). In 8-KO mice, DGAT and TG lipase activities (Fig. 4A,B) as well as DGAT-2 mRNA levels were unchanged whereas TGH and AADA transcript expression (Supporting Fig. 1B) was reduced as compared to WT animals. *In vitro* studies showed that SAMe and 5-aminoimidazole-4-carboxamide-1-β-D-ribofuranoside (AICAR) addition to hepatocytes in culture increased AADA, TGH and DGAT-2 mRNA expression after 6 and 24 hours of treatment (Supporting Fig. 2).

Consistent with the changes recorded in VLDL-TG secretion rate, the MTP TG transfer activity was increased only in mice with NASH (Fig. 4C), whereas no changes were observed in MTP mRNA levels (Supporting Fig. 1C). There was a positive correlation between MTP activity and microsomal TG levels in KO and WT mice ($P < 0.01$, $R = 0.88$) (Supporting

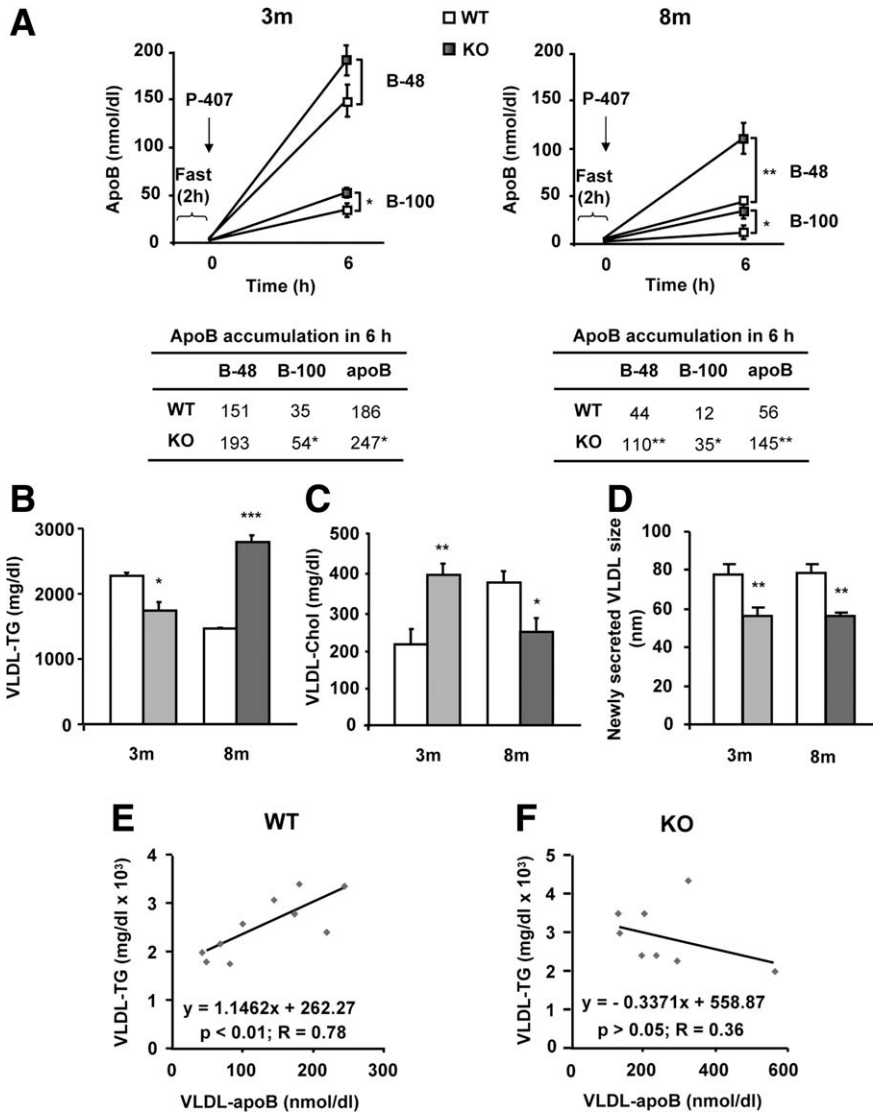

Fig. 2. *MAT1A* deletion increases the rate of VLDL-apoB secretion and impairs VLDL-lipid output in mice. Three-month-old (3m) and 8-month-old (8m) wild type (WT) (□) and *MAT1A*-knockout (*MAT1A*-KO) (■) mice were fasted 2 hours prior to the injection of 1 mg/g poloxamer (P-407) in saline to inhibit VLDL metabolism. Before P-407 injection and 6 hours later, blood was collected and VLDL ($d < 1.02$ g/mL) were isolated from serum by ultracentrifugation and characterized for apoB48, apoB100, triglyceride (TG) and cholesterol (Chol) content and particle size. (A) VLDL-apoB48 (B-48) and VLDL-apoB100 (B-100) mass is represented before and after injection. (B) TG and (C) cholesterol levels were determined in VLDL 6 hours after P-407 injection and corrected with their levels at zero time. (D) Diameters of newly secreted VLDL were measured by dynamic light scattering. For that, hepatocytes isolated from 3m and 8m mice by collagenase digestion were cultured for 24 hours and VLDL isolated from the culture medium. (E,F) Correlation studies were carried out by using Pearson's correlation coefficient and significance was defined as $P < 0.05$. Values are means ± SEM of 4-8 animals per group. Statistical differences between *MAT1A*-KO and WT mice are denoted by $*P < 0.05$, $**P < 0.01$, and $***P < 0.001$ (Student *t* test).

Fig. 3), supporting the concept that microsomal TG concentrations play a role controlling MTP TG transfer activity.

To further assess if *MAT1A* gene has a role in the mobilization of TG for VLDL assembly, lipid turnover studies were performed in primary hepatocytes. We followed cellular lipid synthesis, turnover and secretion from the point of the acyl acceptor (glycerol backbone of glycerolipids) and the acyl donor (fatty acid) by incubating the cells with [^{14}C]glycerol and [^{3}H]oleic acid, exactly as detailed.[10] Hepatocytes from 3-KO mice exhibited a decrease in the [^{3}H]-TG secreted of 35% and 90% in the pulse and the chase periods, respectively, and of 42% in the [^{14}C]-TG secreted during the chase (Fig. 4D). After the chase, the TG content in cells increased (Fig. 4E) whereas its secretion was reduced (Fig. 4F) in 3-KO hepatocytes compared to their controls. Treatment with the adenosine monophosphate–activated protein kinase (AMPK) inhibitor compound c did not recover the disrupted TG mobilization (Supporting Fig. 4).

Increased VLDL-apoB Secretion in 3-Month-Old MAT1A-KO Mice Is Linked to Altered apoB Localization in Hepatocytes But Not to Autophagy Inhibition. ApoB distribution is dramatically altered in 3-KO mice hepatocytes. ApoB accumulates around lipid droplets and looses its reticular distribution. Such localization is more evident in 3-KO hepatocytes challenged with 0.4 mM oleate (Fig. 5A).

We tested whether inhibition of autophagy could underlie the increased VLDL secretion in *MAT1A*-KO mice by analyzing the effect of leupeptin and ammonium chloride on apoB secretion. Inhibition of the lysosomal function, as confirmed by immunoblotting of LC3 (Fig. 5D), was found to decrease VLDL-apoB secretion more markedly in 3-KO hepatocytes (50% and 66% for

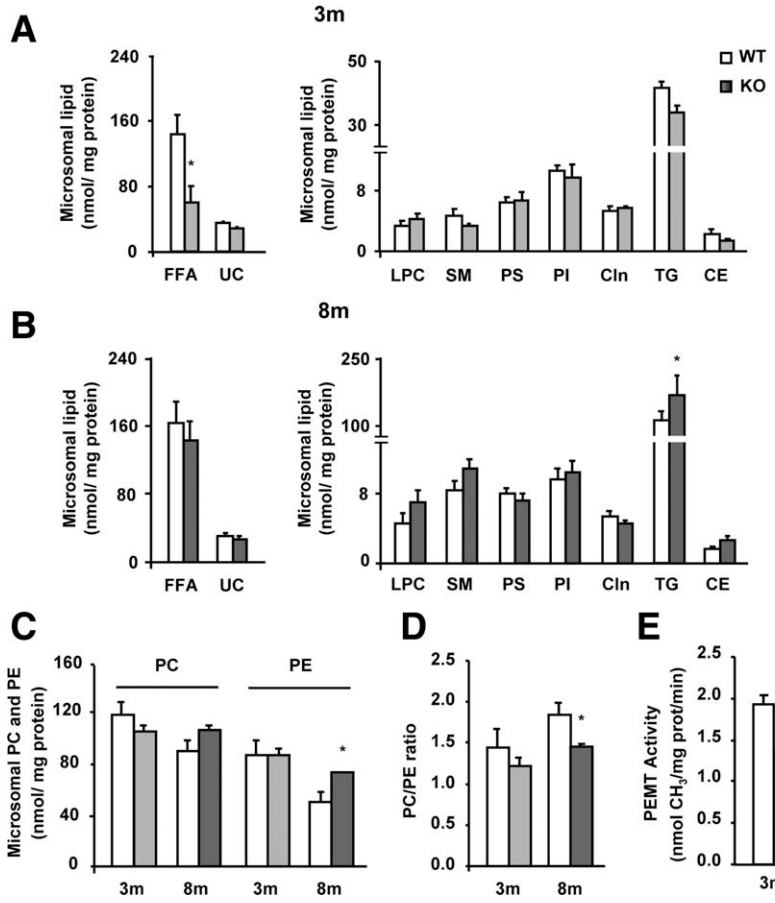

Fig. 3. *MAT1A* deletion alters the microsomal lipid composition in mice. Liver microsomes were isolated from 3-month-old (3m) and 8-month-old (8m) wild type (WT) (□) and *MAT1A*-knockout (*MAT1A*-KO) (■) mice by differential centrifugation. (A-D) Lipids were extracted from liver microsomes, and free fatty acid (FFA), unesterified cholesterol (UC), lysophosphatidylcholine (LPC), sphingomyelin (SM), phosphatidylserine (PS), phosphatidylinositol (PI), cardiolipin (Cln), triglyceride (TG), cholesteryl ester (CE), phosphatidylcholine (PC) and phosphatidylethanolamine (PE) were separated and quantified as indicated in material and methods. (E) Microsomal phosphatidylethanolamine *N*-methyltransferase (PEMT) activity was determined by a radiometric assay. Values are means ± SEM of 4-8 animals per group. Statistical differences between *MAT1A*-KO and WT mice are denoted by $*P < 0.05$ (Student *t* test).

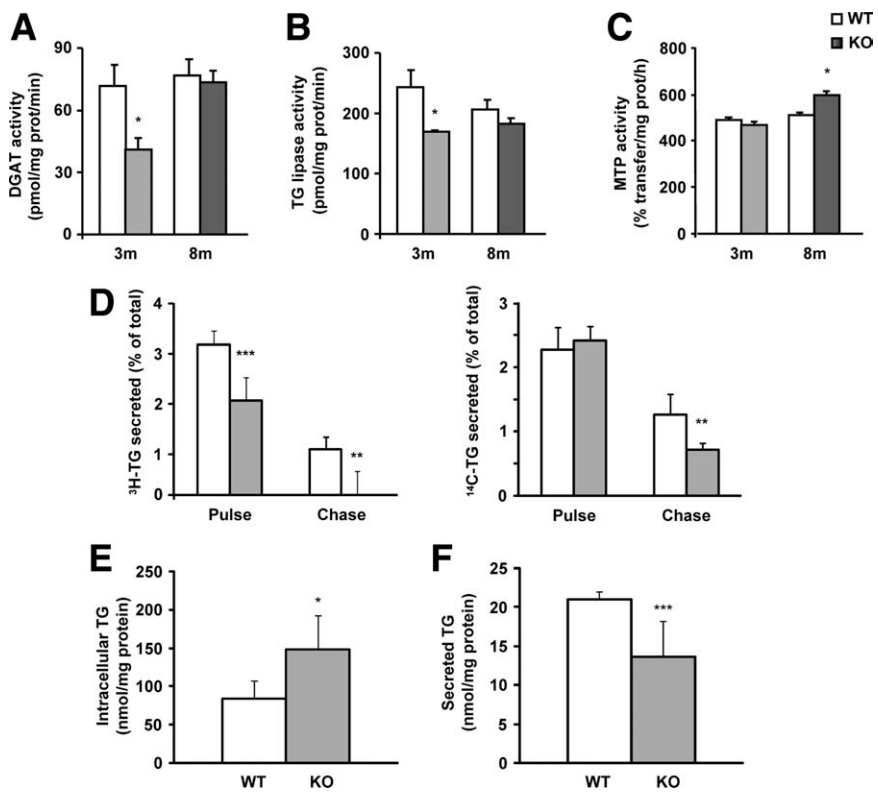

Fig. 4. *MAT1A* deletion decreases the mobilization of triglycerides for VLDL secretion in 3-month-old mice. For enzymatic assays, liver microsomes were prepared from 3-month-old (3m) and 8-month-old (8m) wild type (WT) (□) and *MAT1A*-knockout (*MAT1A*-KO) (■) mice. (A) diacylglycerol acyltransferase (DGAT) and (B) triglyceride (TG) lipase activities were determined by radiometric assays, and the (C) MTP TG transfer activity was measured using a fluorescence assay; all as described in materials and methods. (D-F) 3-month-old mice hepatocytes were incubated 4 hours with 0.4 mM [^{3}H]oleic acid (5 μCi/dish) complexed with 0.5% fatty acid-free BSA and [^{14}C]glycerol (0.5 μCi/dish) (pulse). After a wash of 1 hour in DMEM, cells were incubated for 4 hours (chase). (D) The percentage of the total [^{3}H]-TG and [^{14}C]-TG secreted to the media after both the pulse and chase periods, and the TG content in (E) cells and (F) media after the chase period were calculated. Values are means ± SEM of 4-8 animals per group. Statistical differences between *MAT1A*-KO and WT mice are denoted by $*P < 0.05$, $** P < 0.01$, and $*** P < 0.001$ (Student *t* test).

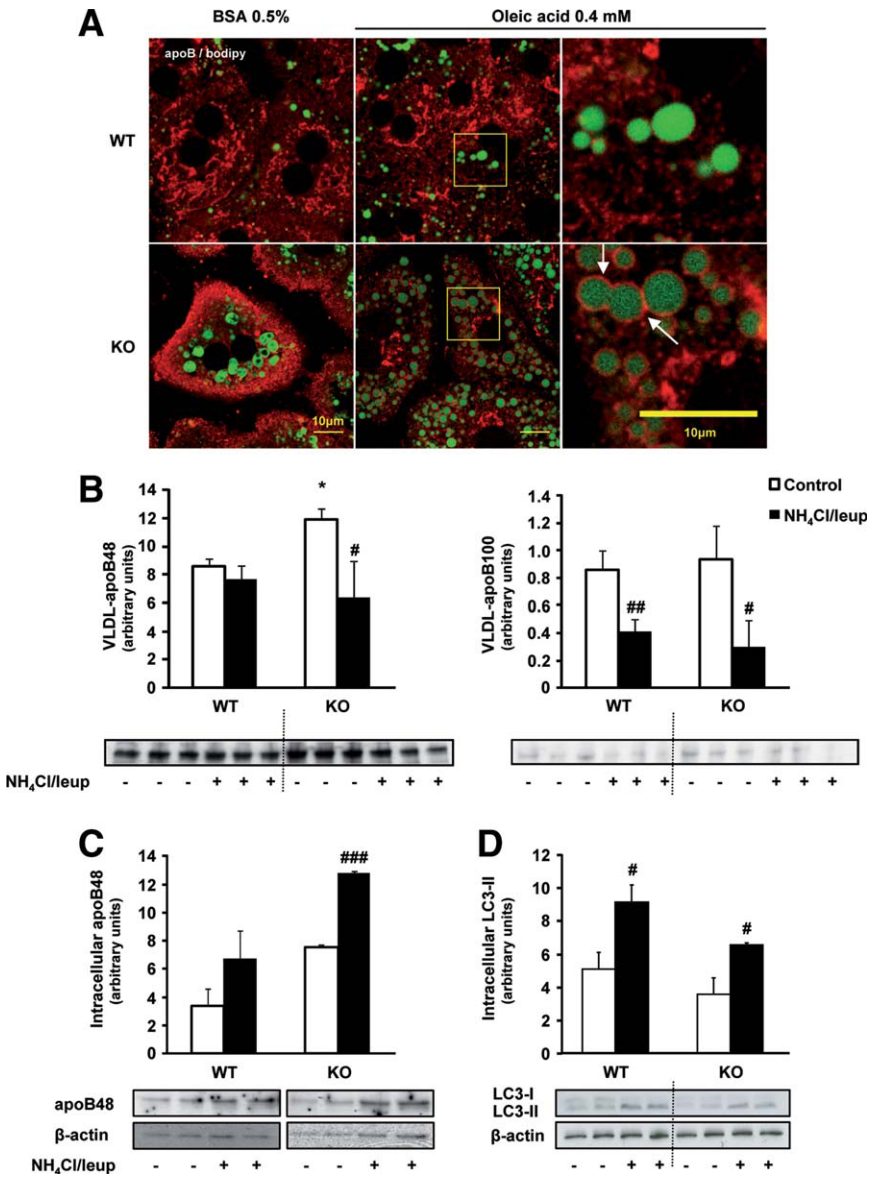

Fig. 5. Increased VLDL-apoB secretion in 3-month-old *MAT1A*-KO mice is linked to altered localization of apoB in hepatocytes but not to autophagy. (A) For confocal laser immunofluorescence analysis of apoB localization in hepatocytes, primary 3-month-old wild-type (WT) and *MAT1A*-knockout (*MAT1A*-KO) mice hepatocytes were incubated for 4 hours in coverslips in DMEM complemented with 0.5% fatty acid–free BSA or 0.4 mM oleic acid in 0.5% BSA. Hepatocytes were then washed with PBS and fixed with 3.7% formaldehyde. After permeabilization (5% Triton X-100), cells were blocked (10% fetal bovine serum in PBS) and double labeled with anti-apoB antibody (red) and BODIPY 493/503 (green). (B-D) Hepatocytes were incubated 24 hours in DMEM without (control, □) or with (■) a mixture of the lysosomal inhibitors leupeptin (100 μM) and ammonium chloride (20 μM). (B) VLDL were isolated from the medium as detailed in material and methods and the VLDL-apoB quantity was analyzed by immunoblotting. (C) Intracellular apoB48 content was assessed by immunoblotting using β-actin as normalizer (apoB100 was not detected). (D) Autophagy was assessed by analysis of the expression of the microtubule-associated proteins, light chain 3-I (LC3-I), and LC3-II by immunoblotting. Statistical differences versus WT mice are denoted by $^*P < 0.05$ and versus control hepatocytes are denoted by $\#P < 0.05$, $\#\#P < 0.01$, and $\#\#\#P < 0.001$ (Student *t* test).

apoB48 and apoB100, respectively) than in 3-WT mice hepatocytes (50% for apoB100) (Fig. 5B) rising the accumulation of apoB mainly in 3-KO hepatocytes (Fig. 5C).

In 3-KO mouse liver, the microsomal lumen apoB content and the cellular [^{35}S]methionine-labeled apoB were increased (Supporting Fig. 4A). MG132 decreased radiolabeled apoB48 in KO mice and had no effect in WT mice (Supporting Fig. 5D). Neither the apoB content in microsomes and microsomal membranes (Supporting Fig. 5B,C) nor the trypsin resistance of apoB were affected by *MAT1A* deletion in 3-month-old mice (Supporting Fig. 5E).

Activation of the PERK-eIF2α Pathway in Liver from MAT1A-Deficient Mice with NASH. To test if the altered lipid and apoB availability induced ER stress, activation of UPR was measured by the phosphorylation degree of PERK and eIF2α. The immunoblots revealed an increase of 1.6- and 2-fold in the ratio of P-PERK and P-eIF2α, versus the total forms, respectively, in 8-KO mice compared to 8-WT mice but not in 3-KO mice (Fig. 6A-C), indicating that the activation of this branch of the UPR occurs only when liver damage is established.

TG and Total Cholesterol Distribution Among Serum Lipoprotein Subclasses Is Disturbed in MAT1A-KO Mice. We analyzed if the smaller size of the secreted VLDL particles in *MAT1A*-KO mice was linked to altered serum lipid distribution among lipoproteins. Our data in 3-KO and 8-KO animals revealed that there is a shift in the maximum peak of VLDL-TG toward particles of smaller diameters (from fraction 5 to 6) (Fig. 7A,B), supporting a decrease in

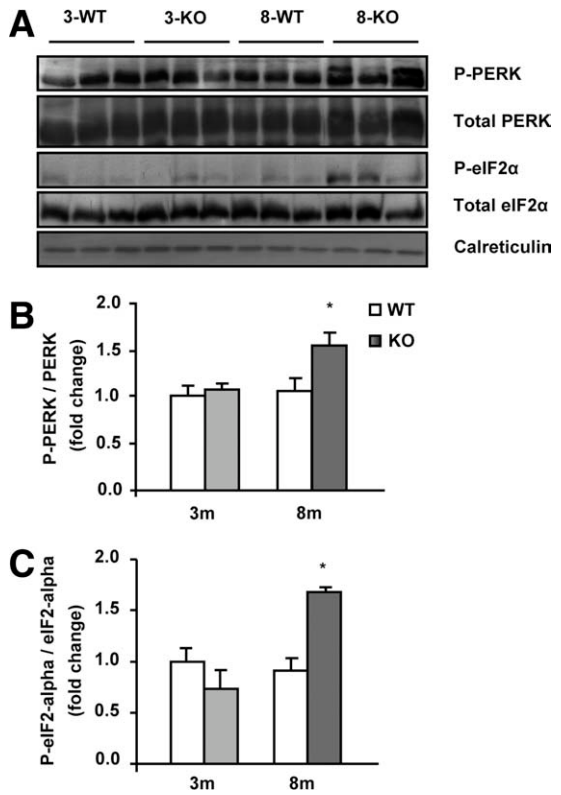

Fig. 6. Activation of the PERK-eIF2α pathway in liver from *MAT1A*-deficient mice with NASH. Liver lysates from 3-month-old (3m) and 8-month-old (8m) wild-type (WT) (□) and *MAT1A*-knockout (*MAT1A*-KO) (■) mice were subjected to 10% dodecyl sulfate-polyacrylamide gel electrophoresis (SDS-PAGE) and proteins were transferred and immobilized on Immobilon-P transfer membranes. Western blotting was performed using primary antibodies for P-eIF2-alpha (ser51), eIF2-alpha, P-PERK (thr980), PERK and calreticulin as normalizer. (A) Representative immunoblots. Fold change over 3-WT for (B) P-PERK and (C) P-eIF2α versus their total forms in *MAT1A*-KO mice and their WT littermates. Values are means ± SEM of 4-8 animals per group. Statistical differences between *MAT1A*-KO and WT mice are denoted by $*P < 0.05$ (Student *t* test).

VLDL size. In addition, *MAT1A* deletion was linked to an increase in the amount of TG associated with LDL subclasses when compared to WT mice, mainly at 3 months of age (Fig. 7A,B). Concerning cholesterol distribution, whereas increased amounts were transported in most LDL subclasses (fractions 8 to 11) in 3-KO and 8-KO mice, lower amounts were transported in several HDL subclasses, with these effects being more marked in 8-KO mice (Fig. 7C,D).

SAMe Recovers VLDL Features and the Activity of Crucial Enzymes Involved in VLDL Assembly in 3-Month-Old MAT1A-KO Mice. Finally, we investigated if the main disorders in VLDL assembly linked to *MAT1A* loss were due to SAMe deficiency. We found that after daily administration of SAMe to 3-KO mice for 7 days, VLDL-apoB secretion decreased even more than the WT values (Fig. 8A), recovering VLDL size and TG and CL content (Fig. 8B,C). Paying attention to the crucial enzyme activities, administration of SAMe to 3-KO mice restored PEMT and DGAT activity in microsomes but did not have any effect over TG lipase (Fig. 8D). SAMe highly decreased KB in serum of 3-KO mice and reestablished FFA levels (Fig. 8E).

Discussion

VLDL secretion is a process of great plasticity for maintaining liver and body lipid homeostasis. It provides a mechanism for controlling intrahepatic TG levels. However, data regarding VLDL-TG secretion in patients with NAFLD showed that even when it increases it does not seem enough to adequately restore the disturbances in liver lipid homeostasis.[4] No previous studies have addressed the question of whether *MAT1A* is required for the assembly and secretion of VLDL. Thus, in the current work we attempted to investigate for the first time the factors that govern VLDL assembly and secretion and its repercussions during NAFLD development in *MAT1A*-KO mice.

Our results showed that with no visible signs of hepatosteatosis in 3-KO mice *MAT1A* deletion caused decreased TG output in VLDL, which was recovered after daily administration of SAMe for 1 week. In contrast, when NASH was established, in 8-KO animals, the total amount of TG secreted in VLDL was higher than in WT. Following a canonical line of thinking,[2,3] our results suggest that the decreased secretion of TG in VLDL at early ages could contribute to the origin of NAFLD, and that the increased TG output in VLDL when NASH is established could be triggered in an unsuccessful attempt to restore lipid homeostasis within the hepatocyte.

Because VLDL-TG secretion rates vary as NAFLD progresses to NASH in *MAT1A*-KO mice, we were curious about the modulation of the mechanisms regulating VLDL assembly at each stage. Several studies have pointed out the relevance of the PEMT pathway to ensure mobilization and export of TG from hepatocytes in VLDL.[20,34] It has also been described that PEMT activity diminishes when the SAMe:SAH ratio decreases and, concomitantly, TG secretion in VLDL.[35] In *MAT1A*-KO mice, the SAMe:SAH ratio is chronically decreased due to hepatic SAMe deficiency.[36] However, although PEMT activity in liver microsomes was lower at 3 months of age recovering after administration of SAMe, it was not at 8 months of age, which suggests that other factors additional to the SAMe:SAH ratio regulate PEMT

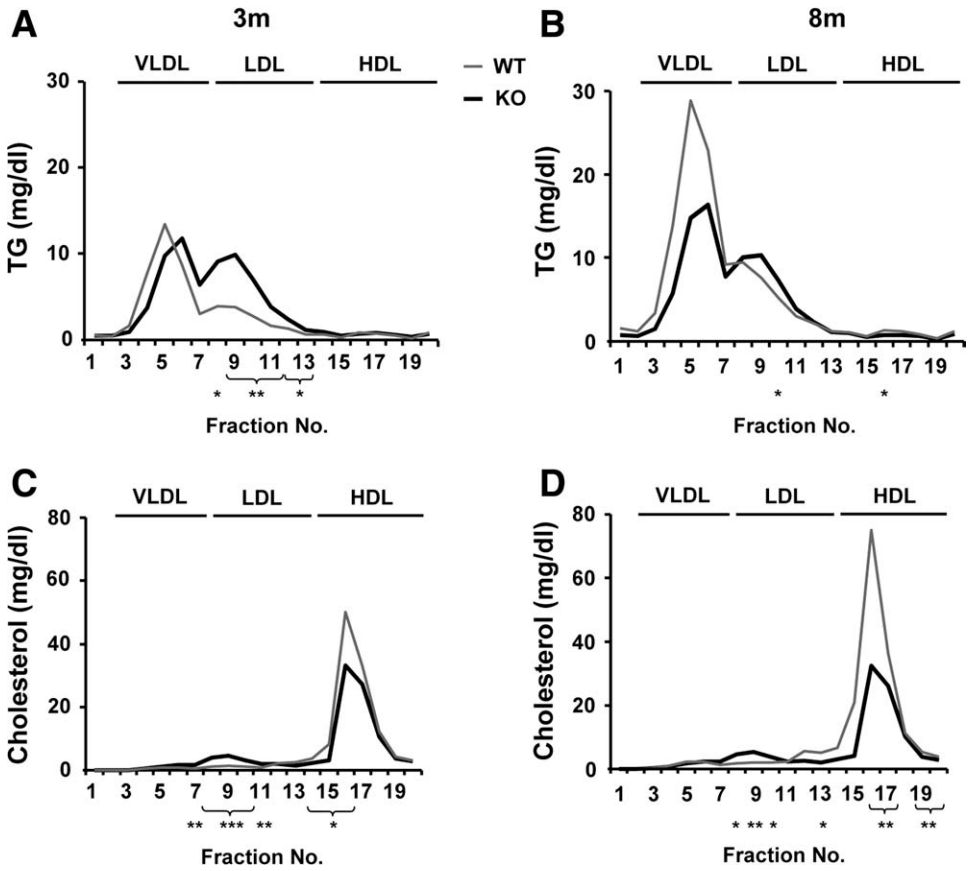

Fig. 7. *MAT1A* deletion alters the triglyceride and total cholesterol distribution among plasma lipoprotein subclasses in mice. Blood was collected from 2 hour fasted 3-month-old (3m) and 8-month-old (8m) wild type (WT) (black line) and *MAT1A*-knockout (*MAT1A*-KO) (gray line) mice. Serum was isolated, and lipoproteins were separated into 20 subclasses (represented as fraction numbers 1 to 20) with gel permeation columns on the basis of differences in particle size by HPLC at Skylight Biotech Inc. (Akita, Japan). (A,B) Triglyceride (TG) and (C,D) total cholesterol concentrations were determined as described in material and methods in the lipoprotein subclasses defined as large (fractions 3-5), medium (fraction 6) and small (fraction 7) VLDL subclasses, large (fraction 8), medium (fraction 9), small (fraction 10) and very small (fractions 11-13) LDL subclasses and very large (fractions 14-15), large (fraction 16), medium (fraction 17), small (fraction 18) and very small (fractions 19-20) HDL subclasses. Values are means ± SEM of 4-8 animals per group. Statistical differences between *MAT1A*-KO and WT mice are denoted by $*P < 0.05$, $**P < 0.01$, and $***P < 0.001$ (Student *t* test).

activity in *MAT1A*-KO mice. A possibility is the higher PE availability in microsomes, which made the PC to PE ratio decrease in 8-KO mice. However, although a decrease in the ratio has been linked to formation of abnormal VLDL particles,[37] the fact that the PC to PE ratio was unchanged in 3-KO mice might suggest a lack of correlation with the changes observed in VLDL assembly in *MAT1A*-KO mice.

The majority (60%-70%) of VLDL-TG secreted from the liver is derived from stored TG via a process of lipolysis and reesterification,[9,10,11,38] and therefore, we focused on the mobilization processes of TG from cytosolic lipid droplets. The 3-KO mice exhibited decreased microsomal TGL and DGAT activity, which recovered after SAMe treatment, as well as reduced microsomal FFA levels and diminished TG turnover and secretion, which could contribute to the origin of hepatosteatosis. Analysis in primary mouse hepatocytes (Supporting Fig. 3) showed that exposure to AICAR (AMPK activator) and SAMe induced the expression of TGH and DGAT-2. Because AMPK is hyperphosphorylated in *MAT1A*-KO mice,[39] we first thought decreased mobilization of TG in *MAT1A*-KO mice could be due to increased AMPK activity. However, treatment with the AMPK inhibitor compound c[40] did not repair the decreased TG mobilization, and thus this hypothesis was discarded. In NASH-affected *MAT1A*-KO mice, eliciting increased VLDL-TG secretion, hepatic TGL and DGAT activity and FFA levels were normal whereas ER stress and the ER resident protein MTP, required for efficient VLDL assembly,[38] were activated.

Regarding cholesterol secretion in VLDL, our data showed that *MAT1A* deletion affected this parameter in a NAFLD stage-specific manner. When NASH was established, decreased VLDL-Chol was found,

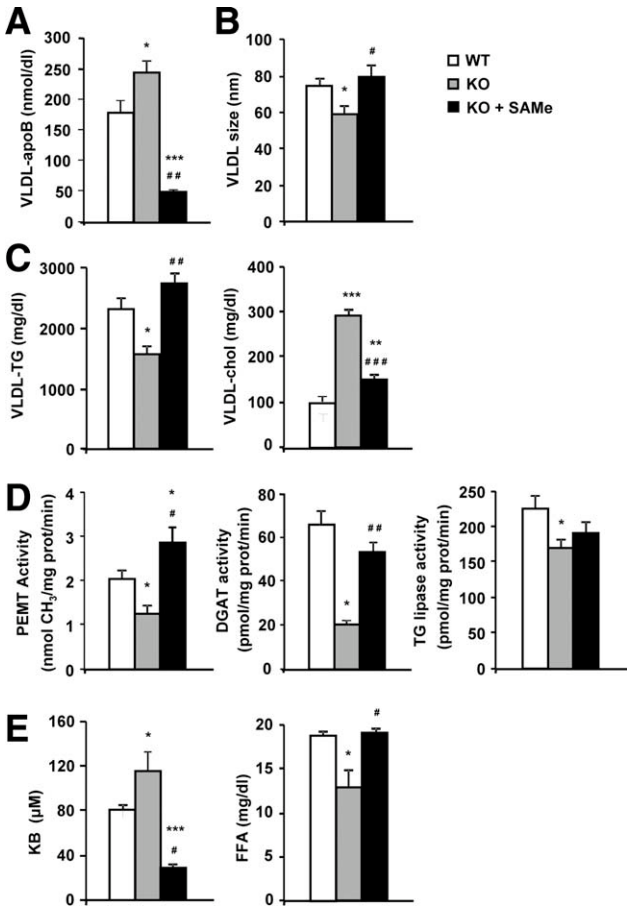

Fig. 8. SAMe recovers VLDL features and the activity of crucial enzymes involved in VLDL assembly in 3-month-old *MAT1A*-KO mice. The 3-month-old wild-type (WT) (□), *MAT1A*-knockout (*MAT1A*-KO) (▩) and SAMe treated *MAT1A*-KO (KO + SAMe) (■) mice were fasted 2 hours prior to the injection of 1 mg/g poloxamer (P-407) in saline to inhibit VLDL metabolism. Before P-407 injection and 6 hours later blood was collected and VLDL (d < 1.02 g/mL) were isolated from serum by ultracentrifugation and characterized for (A) apoB, (B) particle size, (C) triglyceride (TG) and cholesterol (chol) content. (D) Liver microsomes were prepared and microsomal phosphatidylethanolamine *N*-methyltransferase (PEMT), diacylglycerol acyltransferase (DGAT) and TG lipase activities were determined as described in materials and methods. (E) Serum was isolated and levels of ketone bodies (KB) and free fatty acids (FFA) were measured. Values are means ± SEM of 4-8 animals per group. Statistical differences versus WT mice are denoted by $*P < 0.05$, $**P < 0.01$, and $***P < 0.001$ and versus *MAT1A*-KO mice are denoted by $\#P < 0.05$, $\#\#P < 0.01$, and $\#\#\#P < 0.001$ (Student *t* test).

however, at 3 months of age, *MAT1A* deletion was linked to increased cholesterol secretion in VLDL. Based on such findings, we hypothesized that the effect of the loss of function of *MAT1A* on VLDL-lipid metabolism varied depending on lipid availability in the hepatocyte. We suggest that there is a clear effect of *MAT1A* deletion before the establishment of NASH that contributes to the origin of the disease; however, in later stages, other mechanisms related to NASH conduct the molecular events that alter VLDL-lipid metabolism.

A relevant finding in this study is that loss of *MAT1A* gene and the consequent fall in liver SAMe levels increase the number and alter the physical and compositional features of the VLDL particles secreted by the liver which resemble normal after a week of SAMe administration. Because each VLDL particle is built around one molecule of apoB, as a result particles contained less TG and were of smaller diameter than those secreted by WT mouse liver. Similar results were observed in rats treated with LPS,[41] which was reported to inactivate MAT.[42] At both of the studied ages, the maximum peak of TG associated with serum VLDL particles was shifted to the right, providing further evidence for the smaller size of these lipoproteins.

Impaired apoB secretion in VLDL particles could be an interesting issue in NAFLD, because its defective secretion has been linked to the development of ER stress and activation of the PERK-eIF2α pathway.[15] We wanted to find out if *MAT1A* loss in mice affected the availability of apoB within the cell, and if so, whether it was related to UPR activation. Our findings revealed that when UPR was not activated in 3-KO mice, apoB accumulated in the lumen of hepatic microsomes and contained more radiolabeled apoB48 after 2 hours of exposure to [^{35}S]methionine. ApoB is consider to be constitutively synthesized in liver and its secretion to be controlled mainly through posttranslational degradation. ApoB degradation occurs by proteasomal and non proteasomal pathways.[13,14] We wondered if the increased apoB availability was linked to decreased apoB degradation through the proteasomal pathway, and we found that MG132 treatment did not raise [^{35}S]-apoB48 even in WT mice suggesting, as done before for primary rat hepatocytes,[10] that proteasome degradation may not be a main path for apoB degradation in our working model. Recent work proposed that autophagy may be one of the nonproteasomal pathways for apoB degradation[14,43,44] and that apoB accumulation around lipid droplets increased markedly when proteasome activity or autophagy was inhibited.[14] Because apoB was heavily accumulated around lipid droplets in *MAT1A*-KO mice, we wanted to determine whether autophagy inhibition was the cause of the increased VLDL-apoB secretion. To our surprise, we did not find higher increased VLDL-apoB secretion in WT than in KO mice, which could confirm our hypothesis. The results show that inhibition of autophagy decreased VLDL-apoB secretion mainly in 3-KO mice and increased intracellular apoB; this could be taken as a consequence of accumulation of

abnormally lipidated apoB, which cannot be successfully secreted. Thus, increased VLDL-apoB secretion in *MAT1A*-KO mice does not seem to be mediated through inhibition of proteasome or autophagy. Whether other paths engaged in apoB degradation are inactivated, or increased apoB synthesis could occur, remains to be determined.

In conclusion, the findings reported here (Supporting Fig. 7) indicate that *MAT1A* is needed to ensure mobilization of stored TG for VLDL assembly, for maintaining VLDL physical features and for managing apoB availability within the hepatocytes, and reinforce the idea of plasticity of VLDL for maintaining liver and body lipid homeostasis. The results demonstrate that *MAT1A* is required to ensure adequate VLDL assembly and secretion as well as lipoprotein homeostasis.

Acknowledgment: We thank Montse Busto (University of the Basque Country, Bilbao, Spain) for her excellent technical assistance, Olatz Fresnedo (University of the Basque Country, Bilbao, Spain) for her support, Kathleen Botham (The Royal Veterinary College, London, UK) for helpful comments on the manuscript, Marga Esteban (Galdakao Hospital, Bizkaia, Spain) for the serum biochemical analyses, and Servicios Generales de Investigación from the University of the Basque Country, Bilbao, Spain (SGIker) for technical and human support.

References

1. Sundaram M, Yao Z. Recent progress in understanding protein and lipid factors affecting hepatic VLDL assembly and secretion. Nutr Metab (Lond) 2010;7:35.
2. Fujita K, Nozaki Y, Wada K, Yoneda M, Fujimoto Y, Fujitake M, et al. Dysfunctional very-low-density lipoprotein synthesis and release is a key factor in nonalcoholic steatohepatitis pathogenesis. Hepatology 2009;50:772-780.
3. Minehira K, Young SG, Villanueva CJ, Yetukuri L, Oresic M, Hellerstein MK, et al. Blocking VLDL secretion causes hepatic steatosis but does not affect peripheral lipid stores or insulin sensitivity in mice. J Lipid Res 2008;49:2038-2044.
4. Fabbrini E, Sullivan S, Klein S. Obesity and nonalcoholic fatty liver disease: biochemical, metabolic, and clinical implications. Hepatology 2010;51:679-689.
5. Fabbrini E, deHaseth D, Deivanayagam S, Mohammed BS, Vitola BE, Klein S. Alterations in fatty acid kinetics in obese adolescents with increased intrahepatic triglyceride content. Obesity (Silver Spring) 2009;17:25-29.
6. Borchardt RA, Davis RA. Intrahepatic assembly of very low density lipoproteins. Rate of transport out of the endoplasmic reticulum determines rate of secretion. J Biol Chem 1987;262:16394-16402.
7. Dixon JL, Furukawa S, Ginsberg HN. Oleate stimulates secretion of apolipoprotein B-containing lipoproteins from Hep G2 cells by inhibiting early intracellular degradation of apolipoprotein B. J Biol Chem 1991;266:5080-5086.
8. Gibbons GF, Khurana R, Odwell A, Seelaender MC. Lipid balance in HepG2 cells: active synthesis and impaired mobilization. J Lipid Res 1994;35:1801-1808.
9. Wiggins D, Gibbons GF. The lipolysis/esterification cycle of hepatic triacylglycerol. Its role in the secretion of very-low-density lipoprotein and its response to hormones and sulphonylureas. Biochem J 1992; 284:457-462.
10. Gilham D, Ho S, Rasouli M, Martres P, Vance DE, Lehner R. Inhibitors of hepatic microsomal triacylglycerol hydrolase decrease very low density lipoprotein secretion. FASEB J 2003;17:1685-1687.
11. Yang LY, Kuksis A, Myher JJ, Steiner G. Contribution of de novo fatty acid synthesis to very low density lipoprotein triacylglycerols: evidence from mass isotopomer distribution analysis of fatty acids synthesized from [2H6]ethanol. J Lipid Res 1996;36:125-136.
12. Hussain MM, Shi J, Dreizen P. Microsomal triglyceride transfer protein and its role in apoB-lipoprotein assembly. J Lipid Res 2003;44:22-32.
13. Benoist F, Grand-Perret T. Co-translational degradation of apolipoprotein B100 by the proteasome is prevented by microsomal triglyceride transfer protein. Synchronized translation studies on HepG2 cells treated with an inhibitor of microsomal triglyceride transfer protein. J Biol Chem 1997;272:20435-20442.
14. Ohsaki Y, Cheng J, Fujita A, Tokumoto T, Fujimoto T. Cytoplasmic lipid droplets are sites of convergence of proteasomal and autophagic degradation of apolipoprotein B. Mol Biol Cell 2006;17:2674-2683.
15. Su Q, Tsai J, Xu E, Qiu W, Bereczki E, Santha M, et al. Apolipoprotein B100 acts as a molecular link between lipid-induced endoplasmic reticulum stress and hepatic insulin resistance. Hepatology 2009;50: 77-84.
16. Gentile CL, Pagliassotti MJ. The endoplasmic reticulum as a potential therapeutic target in nonalcoholic fatty liver disease. Curr Opin Investig Drugs 2008;9:1084-1088.
17. Ota T, Gayet C, Ginsberg HN. Inhibition of apolipoprotein B100 secretion by lipid-induced hepatic endoplasmic reticulum stress in rodents. J Clin Invest 2008;118:316-332.
18. Yao ZM, Vance DE. The active synthesis of phosphatidylcholine is required for very low density lipoprotein secretion from rat hepatocytes. J Biol Chem 1988;263:2998-3004.
19. Jacobs RL, Devlin C, Tabas I, Vance DE. Targeted deletion of hepatic CTP:phosphocholine cytidylyltransferase alpha in mice decreases plasma high density and very low density lipoproteins. J Biol Chem 2004;279:47402-47410.
20. Noga AA, Zhao Y, Vance DE. An unexpected requirement for phosphatidylethanolamine N-methyltransferase in the secretion of very low density lipoproteins. J Biol Chem 2002;277:42358-42365.
21. Cabrero C, Duce AM, Ortiz P, Alemany S, Mato JM. Specific loss of the high-molecular-weight form of S-adenosyl-L-methionine synthetase in human liver cirrhosis. Hepatology 1988;8:1530-1534.
22. Duce AM, Ortiz P, Cabrero C, Mato JM. S-adenosyl-L-methionine synthetase and phospholipid methyltransferase are inhibited in human cirrhosis. Hepatology 1988;8:65-68.
23. Mato JM, Lu SC. Role of S-adenosyl-L-methionine in liver health and injury. Hepatology 2007;45:1306-1312.
24. Vendemiale G, Altomare E, Trizio T, Le Grazie C, Di Padova C, Salerno MT, et al. Effects of oral S-adenosyl-L-methionine on hepatic glutathione in patients with liver disease. Scand J Gastroenterol 1989;24:407-415.
25. Lu SC, Alvarez L, Huang ZZ, Chen L, An W, Corrales FJ, et al. Methionine adenosyltransferase 1A knockout mice are predisposed to liver injury and exhibit increased expression of genes involved in proliferation. Proc Natl Acad Sci U S A 2001;98:5560-5565.
26. Tomasi ML, Ramani K, Lopitz-Otsoa F, Rodriguez MS, Li TW, Ko K, et al. S-adenosylmethionine regulates dual-specificity mitogen-activated protein kinase phosphatase expression in mouse and human hepatocytes. Hepatology 2010;51:2152-2161.
27. Ruiz JI, Ochoa B. Quantification in the subnanomolar range of phospholipids and neutral lipids by monodimensional thin-layer chromatography and image analysis. J Lipid Res 1997;38:1482-1489.
28. Bligh EG, Dyer WJ. A rapid method of total lipid extraction and purification. Can J Biochem Physiol 1959;37:911-917.
29. Cano A, Ciaffoni F, Safwat GM, Aspichueta P, Ochoa B, Bravo E, et al. Hepatic VLDL assembly is disturbed in a rat model of

nonalcoholic fatty liver disease: is there a role for dietary coenzyme Q? J Appl Physiol 2009;107:707-717.
30. Cristobal S, Ochoa B, Fresnedo O. Purification and properties of a cholesteryl ester hydrolase from rat liver microsomes. J Lipid Res 1999; 40:715-725.
31. Dolinsky VW, Douglas DN, Lehner R, Vance DE. Regulation of the enzymes of hepatic microsomal triacylglycerol lipolysis and re-esterification by the glucocorticoid dexamethasone. Biochem J 2004;378: 967-974.
32. Ridgway ND, Vance DE. Phosphatidylethanolamine N-methyltransferase from rat liver. Methods Enzymol 1992;209:366-374.
33. Bartolomé N, Aspichueta P, Martínez MJ, Vázquez-Chantada M, Martínez-Chantar ML, Ochoa B, et al. Biphasic adaptative responses in VLDL metabolism and lipoprotein homeostasis during Gram-negative endotoxemia. Innate Immun 2010; doi:10.1177/1753425910390722.
34. Kharbanda KK, Todero SL, Ward BW, Cannella JJ 3rd, Tuma DJ. Betaine administration corrects ethanol-induced defective VLDL secretion. Mol Cell Biochem 2009;327:75-78.
35. Kharbanda KK, Mailliard ME, Baldwin CR, Beckenhauer HC, Sorrell MF, Tuma DJ. Betaine attenuates alcoholic steatosis by restoring phosphatidylcholine generation via the phosphatidylethanolamine methyltransferase pathway. J Hepatol 2007;46:314-321.
36. Mato JM, Martínez-Chantar ML, Lu SC. Methionine metabolism and liver disease. Annu Rev Nutr 2008;28:273-293.
37. Fast DG, Vance DE. Nascent VLDL phospholipid composition is altered when phosphatidylcholine biosynthesis is inhibited: evidence for a novel mechanism that regulates VLDL secretion. Biochim Biophys Acta 1995;1258:159-168.
38. Gibbons GF, Wiggins D, Brown AM, Hebbachi AM. Synthesis and function of hepatic very-low-density lipoprotein. Biochem Soc Trans 2004;32:59-64.
39. Vázquez-Chantada M, Ariz U, Varela-Rey M, Embade N, Martínez-Lopez N, Fernández-Ramos D, et al. Evidence for LKB1/AMP-activated protein kinase/endothelial nitric oxide synthase cascade regulated by hepatocyte growth factor, S-adenosylmethionine, and nitric oxide in hepatocyte proliferation. HEPATOLOGY 2009;49:608-617.
40. Rencurel F, Foretz M, Kaufmann MR, Stroka D, Looser R, Leclerc I, et al. Stimulation of AMP-activated protein kinase is essential for the induction of drug metabolizing enzymes by phenobarbital in human and mouse liver. Mol Pharmacol 2006;70:1925-1934.
41. Aspichueta P, Pérez S, Ochoa B, Fresnedo O. Endotoxin promotes preferential periportal upregulation of VLDL secretion in the rat liver. J Lipid Res 2005;46:1017-1026.
42. Ko K, Yang H, Noureddin M, Iglesia-Ara A, Xia M, Wagner C, et al. Changes in S-adenosylmethionine and GSH homeostasis during endotoxemia in mice. Lab Invest 2008;88:1121-1129.
43. Pan M, Maitin V, Parathath S, Andreo U, Lin SX, St Germain C, et al. Presecretory oxidation, aggregation, and autophagic destruction of apoprotein-B: a pathway for late-stage quality control. Proc Natl Acad Sci U S A 2008;105:5862-5867.
44. Zhong S, Magnolo AL, Sundaram M, Zhou H, Yao EF, Di Leo E, et al. Nonsynonymous mutations within APOB in human familial hypobetalipoproteinemia: evidence for feedback inhibition of lipogenesis and postendoplasmic reticulum degradation of apolipoprotein B. J Biol Chem 2010;285:6453-6464.